

RESCEU-32/99 UTAP-343/99

Density Profiles of Dark Matter Halo are not Universal

Y.P. Jing and Yasushi Suto

Department of Physics and Research Center for the Early Universe (RESCEU)
 School of Science, University of Tokyo, Tokyo 113-0033, Japan.
 jing@utap.phys.s.u-tokyo.ac.jp, suto@phys.s.u-tokyo.ac.jp

ABSTRACT

We perform a series of high – resolution N-body simulations designed to examine the density profiles of dark matter halos. From 12 simulated halos ranging the mass of $2 \times 10^{12} \sim 5 \times 10^{14} h^{-1} M_{\odot}$ (represented by ~ 1 million particles within the virial radius), we find a clear systematic correlation between the halo mass and the slope of the density profile at 1% of the virial radius, in addition to the variations of the slope among halos of the similar mass. More specifically, the slope is ~ -1.5 , -1.3 , and -1.1 for galaxy, group, and cluster mass halos, respectively. In addition to the fact that we confirmed the earlier simulation results that the inner slope is steeper than the *universal* profile originally proposed by Navarro, Frenk & White, this mass dependence is inconsistent with the several analytical arguments attempting to link the inner slope with the primordial index of the fluctuation spectrum. Thus we conclude that the dark matter density profiles, especially in the inner region, are not universal.

Subject headings: galaxies: clusters: general – cosmology: miscellaneous – methods: numerical

1. Introduction

Can one recover (some aspects of) the initial condition of the universe from the distribution of galaxies at $z \sim 0$? A conventional answer to this question is affirmative, *provided* that the effect of a spatial bias is reasonably understood and/or if it does not significantly alter the interpretation of the observed distribution. This consensus underlies the tremendous effort in the past and at present to extract the cosmological implications

from the existing and future galaxy redshift surveys. The two-point correlation function $\xi(r)$ is a good example supporting this idea; on large scales it is trivially related to the primordial spectrum of mass fluctuations, $P_i(k)$. Furthermore the effective power-law index of the two-point correlation function on sufficiently small scales is related to the initial power-law index n_i of $P_i(k) \propto k^{n_i}$ as $\xi(r) \propto r^{-3(3+n_i)/(5+n_i)}$ (Peebles(1980), Sugino et al.(1991), Suto(1993)). In other words, the initial condition of the universe is imprinted in the behavior of galaxies on small scales (again apart from the effect of bias). This is why the phenomenological fitting formula for the nonlinear power spectrum (Hamilton et al.(1991), Jain, Mo, & White (1995), Peacock & Dodds(1996), Ma (1998)) turned out to be so successful. On the other hand, it is clearly hopeless to extract any meaningful cosmological information from the precise data on the orbit of the earth around the Sun; all the initial memory is supposed to be completely lost due to the strongly nonlinear and chaotic nature of the gravitation (see, e.g., Suto 1991).

These two results are not inconsistent with each other, of course. The two-point correlation function of galaxies is estimated via statistical averaging over many galaxy pairs, describes clustering on $\sim (0.1 - 10)h^{-1}\text{Mpc}$ scales, and thus is not necessarily limited to a virialized system. In contrast, the earth around the Sun merely provides one realization (and thus no statistical information available) for a strongly bound pair of separation of $\sim 10^{-13}\text{Mpc}$! Thus it is not surprising that those two examples show a completely different degree of the dependence on the initial conditions of the universe. Nevertheless, they clearly exhibit the difficulty in interpreting and understanding the reality and origin of the universal density profile proposed by Navarro, Frenk & White (1996,1997; hereafter NFW); dark matter halos are virialized (at least NFW selected such halos), their relevant scales are $\sim (0.01 - 1)h^{-1}\text{Mpc}$, and they should have experienced different merging histories depending on their environment and mass. Thus even if they do have a *universal* density profile *statistically* (i.e., after averaging over many realizations), it is also natural that individual halo profiles are intrinsically scattered around the universal profile (Jing(1999)). Definitely this is a matter of semantics to a certain extent; the most important finding of NFW is that such halo-to-halo variations are surprisingly small.

A universal density profile was also reported by Moore et al.(1999) on the basis of high – resolution simulations of one cluster-mass halo and four galaxy-mass halos, and they claim that the density profile $\rho(r) \propto r^{-1.5}$ in the most inner region. In what follows, we will address the following quantitative and specific questions concerning the halo profile, especially its most inner region, using the high-resolution N -body simulations; the inner slope of the halo profile is really described by $\rho(r) \propto r^{-1}$ or $\rho(r) \propto r^{-1.5}$ *universally* as NFW and Moore et al.(1999) claimed ? If not, does the slope vary among the different halos ? Is there any systematic correlation between the slope and the mass of halos ?

In fact, some of the above questions have been partially addressed previously with different approaches and methodologies (Fukushige & Makino(1997), Evans & Collet(1997), Moore et al.(1998), Syer & White(1998), Nusser & Sheth(1999), Jing(1999), Avila-Reese et al.(1999), Bullock et al.(1999)). In order to revisit those in a more systematic and unambiguous manner, we have developed a nested grid P^3M N-body code designed to the current problem so as to ensure the required numerical resolution in the available computer resources. This enables us to simulate 12 realizations of halos in a low-density cold dark matter (Λ CDM) universe with $(0.5 - 1) \times 10^6$ particles in a range of mass $10^{12 \sim 15} M_\odot$.

2. Simulation procedure

As Fukushige & Makino(1997) and later Moore et al.(1998) demonstrated, the inner profile of dark matter halos is substantially affected by the mass resolution of simulations. To ensure the required resolution (at least comparable to theirs), we adopt the following two-step procedure. A detailed description of the implementation and resolution test will be presented elsewhere.

First we select dark matter halos from our previous cosmological P^3M N-body simulations with 256^3 particles in a $(100h^{-1}\text{Mpc})^3$ cube (Jing & Suto(1998), Jing(1998)). To be specific, we use one simulation of the Λ CDM model of $\Omega_0 = 0.3$, $\lambda_0 = 0.7$, $h = 0.7$ and $\sigma_8 = 1.0$ according to Kitayama & Suto(1997). The mass of the individual particle in this simulation is $7 \times 10^9 M_\odot$. The candidate halo catalogue is created using the friend-of-friend grouping algorithm with the bonding length of 0.2 times the mean particle separation.

We choose twelve halos in total from the candidate catalogue so that they have mass scales of clusters, groups, and galaxies (Table 1). Except for the mass range, the selection is random, but we had to exclude about 40% halos of galactic mass from the original candidates since they have a neighboring halo with a much larger mass. We use the multiple mass method to re-simulate them. To minimize the contamination of the coarse particles on the halo properties within the virial radius at $z = 0$, r_{vir} , we trace back the particles within $3r_{\text{vir}}$ of each halo to their initial conditions at redshift $z = 72$. This is more conservative than that adopted in previous studies, and in fact turned out to be important for galactic mass halos. Note that we define r_{vir} such that the spherical overdensity inside is $\sim 18\pi^2\Omega_0^{0.4} \sim 110$ times the critical density, $\rho_{\text{crit}}(z = 0)$.

Then we regenerate the initial distribution in the cubic volume enclosing these halo particles with larger number of particles by adding shorter wavelength perturbation to the

identical initial fluctuation of the cosmological simulation. Next we group fine particles into coarse particles (consisting of at most 8 fine particles) within the high-resolution region if they are not expected to enter the central halo region within $3r_{\text{vir}}$. As a result, there are typically 2.2×10^6 simulation particles, $\sim 1.5 \times 10^6$ fine particles and $\sim 0.7 \times 10^6$ coarse particles for each halo. Finally about $(0.5 - 1) \times 10^6$ particles end up within r_{vir} of each halo. Note that this number is significantly larger than those of NFW, and comparable to those of Fukushige & Makino(1997) and Moore et al.(1998), Moore et al.(1999).

We evolve the initial condition for the selected halo generated as above using a new code developed specifically for the present purpose. The code implements the nested-grid refinement feature in the original P³M N-body code of Jing & Fang(1994). Our code implements a constant gravitational softening length in comoving coordinates, and we change its value at $z = 4, 3, 2$, and 1 so that the proper softening length (about 3 times the Plummer softening length) becomes $0.005 r_{200}$, where r_{200} is the radius within which the spherical overdensity is $200\rho_{\text{crit}}(z = 0)$. Thus our simulations effectively employ the constant softening length in proper coordinates at $z \leq 4$. The first refinement is placed to include all fine particles, and the particle-particle (PP) short range force is added to compensate for the larger softening of the particle-mesh (PM) force. When the CPU time of the PP computation exceeds twice the PM calculation as the clustering develops, a second refinement is placed around the center of the halo with the physical size about 1/3 of that of the first refinement. The mesh size is fixed to 360^3 for the parent periodic mesh and for the two isolated refinements. The CPU time for each step is about 1.5 minutes at the beginning and increases to 5 minutes at the final epoch of the simulation on one vector processor of Fujitsu VPP300 (peak CPU speed of 1.6 GFLOPS). A typical run of 10^4 time steps, which satisfies the stability criteria (Pearce et al. 1995), takes 700 CPU hours to complete.

3. Results

Figure 1 displays the snapshot of the twelve halos at $z = 0$. Clearly all the halos are far from spherically symmetric, and surrounded by many substructures and merging clumps. This is qualitatively similar to that found by Moore et al.(1998), Moore et al.(1999) for their high-resolution halos in the $\Omega_0 = 1$ CDM model. The corresponding radial density profiles are plotted in Figure 2. The halo center is defined as the potential minimum. In spite of the existence of apparent sub-clumps (Fig. 1), the spherically averaged profiles are quite smooth and similar to each other as first pointed out by NFW. The inner slope of the profiles, however, is generally steeper than the NFW value, -1 , in agreement with the previous findings of Fukushige & Makino(1997) and Moore et al.(1998). We have

fitted the profiles to $\rho(r) \propto r^{-1.5}(r + r_s)^{-1.5}$ (Moore et al. 1999; the solid curves) and $\rho(r) \propto r^{-1}(r + r_s)^{-2}$ (NFW; the dotted curves) for $0.01r_{200} \leq r \leq r_{200}$. The resulting concentration parameter c , defined as the r_{200}/r_s , is plotted in the left panel of Figure 3. This is the most accurate determination of the concentration parameter for the LCDM model. There exists a significant scatter among c for similar mass (Jing(1999)), and a clear systematic dependence on halo mass (NFW, Moore et al.(1999)).

The most important result is that the density profiles of the 4 galactic halos are all well fitted to the Moore et al.(1999) form, but those of the cluster halos are better fitted to the NFW form. This is in contrast with Moore et al.(1999) who concluded that both galactic and cluster halos have the universal density profile $\rho(r) \propto r^{-1.5}(r + r_s)^{-1.5}$, despite that they considered one cluster-mass halo alone. In fact, our current samples can address this question in a more statistical manner. CL1 has significant substructures, and the other three are nearly in equilibrium. Interestingly the density profiles of CL2 and CL3 are better fitted to the NFW form, and that of CL4 is in between the two forms. The density profiles of the group halos are in between the galactic and cluster halos, as expected. One is better fitted to the NFW form, but the other three, to the Moore et al.(1999) form.

To examine this more quantitatively, we plot the inner slope fitted to a power-law for $0.007 < r/r_{200} < 0.02$ as a function of the halo mass in the right panel of Figure 3. This figure indicates two important features; a significant scatter of the inner slope among the halos with similar masses and a clear systematic trend of the steeper profile for the smaller mass. For reference we plot the predictions for the slope, $-3(3+n)/(4+n)$ by Hoffman & Shaham(1985) and $-3(3+n)/(5+n)$ by Syer & White(1998), using the effective power-law index n_{eff} of the linear power spectrum at the corresponding mass scale for n (Table 1). With a completely different methodology, Nusser & Sheth(1999) argue that the slope of the density profile within $\sim 0.01r_{\text{vir}}$ is in between the above two values. On the basis of the slope – mass relation that we discovered, we disagree with their interpretation; for the galactic halos, the analytical predictions could be brought into agreement with our simulation only if the effective slope were -2 , which is much larger than the actual value -2.5 on the scale.

We would like to emphasize that our results are robust against the numerical resolution for the following reasons. Since we have used the same time steps and the same force softening length in terms of r_{200} , the resolution effect, which is generally expected to make the inner slope of $\rho(r)$ shallower, should influence the result of the galactic halos more than that of cluster halos. In fact this is opposite to what we found in the simulation. Furthermore our high-resolution simulation results agree very well with those of the lower-resolution cosmological simulations (open triangles) for the cluster halos on scales

larger than their force softening length (short thin lines at the bottom of Figure 2). We have also repeated the simulations of several halos employing 8 times less particles and 2 times larger softening length, and made sure that the force softening length $\sim 0.005r_{200}$ (the vertical dashed lines of Figure 2) is a good indicator for the resolution limit.

4. Conclusion

In this *Letter* we have presented by far the most reliable and systematic study on the dark matter density profiles. This is the first study which simulates a dozen of dark halos with about a million particles in a flat low-density CDM universe. This enables us to address the profile of the halos with unprecedented accuracy and statistical reliability. While qualitative aspects of our results are not inconsistent with those reported by Moore et al. (1999), our larger sample of halos provided convincing evidence that *the form* of the density profiles is not universal.

As a matter of fact, it is not easy to explain the behavior analytically. Although the analytical work (Syer & White(1998), Nusser & Sheth(1999), Lokas(1999)) concluded that the inner profile should be steeper than -1 , their interpretation and/or predicted mass-dependence are different from our numerical results. This implies that while their arguments may cover some parts of the physical effects, they do not fully account for the intrinsically complicated nonlinear dynamical evolution of non-spherical self-gravitating systems. We note that the inner slope of the halo profile is essentially determined by the central density of the halo which would have been formed first. Statistically smaller objects should collapse and virialize earlier than more massive ones, and thus it is natural that the central density becomes smaller for more massive halos. If the outer density is regulated by cosmological evolution independently of the the central region, it would explain the mass dependence of the inner slope that we found. Alternatively, the scaling in terms of r_{200} irrespective of the mass of halos, which we have been implicitly assumed here, may be broken; in that case the comparison of the slope of halos at $0.01r_{200}$ would not make sense, and this might produce the mass dependence. Figure 3, however, seems to indicate that r_s , which would provide a more natural length-scale of an individual halo, is almost proportional to r_{200} . Thus the scaling of halos in terms of r_{200} may not be a bad approximation in practice.

In summary, the mass dependence of the inner profile indicates the difficulty in understanding the halo density profile from the cosmological initial conditions in a straightforward manner. Even if the density profiles of dark halos are not universal to the extent which NFW claimed, however, they definitely deserves further investigation from

both numerical and analytical points of view.

We thank J. Makino for many stimulating discussions and suggestions. Y.P.J. gratefully acknowledges support from a JSPS (Japan Society for the Promotion of Science) fellowship. Numerical computations were carried out on VPP300/16R and VX/4R at ADAC (the Astronomical Data Analysis Center) of the National Astronomical Observatory, Japan, as well as at RESCEU (Research Center for the Early Universe, University of Tokyo) and KEK (High Energy Accelerator Research Organization, Japan). This research was supported in part by the Grant-in-Aid by the Ministry of Education, Science, Sports and Culture of Japan (07CE2002) to RESCEU, and by the Supercomputer Project (No.99-52) of KEK.

REFERENCES

Avila-Reese, V., Firmani, C., Klypin, A., Kravtsov, A.V. 1999, astro-ph/9906260
Bullock, J.S. et al. 1999, ApJ, submitted (astro-ph/9908159)
Couchman, H.M.P., Thomas, P.A., & Pearce, F.R. 1995, ApJ, 452, 797
Eke, V.R, Navarro, J.F., & Frenk, C.S. 1998, ApJ, 503, 569
Evans, N.W. & Collett, J.L. 1997, ApJ, 480, L103
Fukushige, T., & Makino, J. 1997, ApJ, 477, L9
Hamilton, A.J.S., Kumar, P., Lu, E., & Matthews, A. 1991, ApJ, 374, L1
Hoffman, Y., & Shaham, J. 1985, ApJ, 297, 16
Jain, B., Mo, H.J., & White, S.D.M. 1995, MNRAS, 276, 25
Jing, Y. P. 1998, ApJ, 494, L5
Jing, Y. P. 1999, ApJ, submitted (astro-ph/9901340)
Jing, Y.P. & Fang, L.Z. 1994, ApJ, 432, 438
Jing, Y.P. & Suto, Y. 1998, ApJ, 494, L5
Kitayama, T. & Suto, Y. 1997, ApJ, 490, 557
Lokas, E.L. 1999, MNRAS, in press (astro-ph/9901185)
Ma, C.-P. 1998, ApJ, 508, L5
Moore, B., Governato, F., Quinn, T., Stadel, J., & Lake, G. 1998, ApJ, 499, L5
Moore, B., Quinn, T., Governato, F., Stadel, J., & Lake, G. 1999, MNRAS, submitted, astro-ph/9903164
Navarro, J.F., Frenk, C.S., & White, S.D.M. 1996, ApJ, 462, 563
Navarro, J.F., Frenk, C.S., & White, S.D.M. 1997, ApJ, 490, 493
Nusser, A., & Sheth, R.K. 1999, MNRAS, 303, 685
Peacock, J.A. & Dodds, S.J. 1996, MNRAS, 280, L19

Peebles, P.J.E. 1980, The Large Scale Structure of the Universe (Princeton University Press: Princeton)

Suginohara, T., Suto, Y., Bouchet, F.R., & Hernquist, L. 1991, ApJS, 75, 631

Suto, Y. 1991, PASJ, 43, L9

Suto, Y. 1993, Prog.Theor.Phys., 90, 1173

Syer, D., & White, S.D.M. 1998, MNRAS, 293, 337

Table 1. Properties of the simulated halos

halo ID	M [$h^{-1}M_{\odot}$] ^a	No. of particles ^b	$r_{200}[h^{-1}\text{Mpc}]$ ^c	$r_{\text{vir}}[h^{-1}\text{Mpc}]$ ^d	n_{eff} ^e
GX 1	2.30×10^{12}	458,440	0.197	0.269	-2.47
GX 2	5.31×10^{12}	840,244	0.265	0.356	-2.42
GX 3	4.21×10^{12}	694,211	0.242	0.330	-2.44
GX 4	5.60×10^{12}	1,029,895	0.275	0.363	-2.42
GR 1	4.66×10^{13}	772,504	0.544	0.735	-2.31
GR 2	4.68×10^{13}	907,489	0.502	0.736	-2.31
GR 3	5.24×10^{13}	831,429	0.561	0.764	-2.30
GR 4	5.12×10^{13}	901,518	0.576	0.758	-2.30
CL 1	4.77×10^{14}	522,573	1.15	1.59	-2.12
CL 2	3.36×10^{14}	839,901	1.04	1.42	-2.14
CL 3	2.89×10^{14}	664,240	1.00	1.35	-2.16
CL 4	3.17×10^{14}	898,782	1.06	1.39	-2.15

^aMass of the halo within its virial radius.

^bNumber of particles within its virial radius.

^cthe radius within which the spherical overdensity is 200 times the critical density.

^dthe virial radius.

^ethe effective slope of the linear power spectrum at the halo mass scale

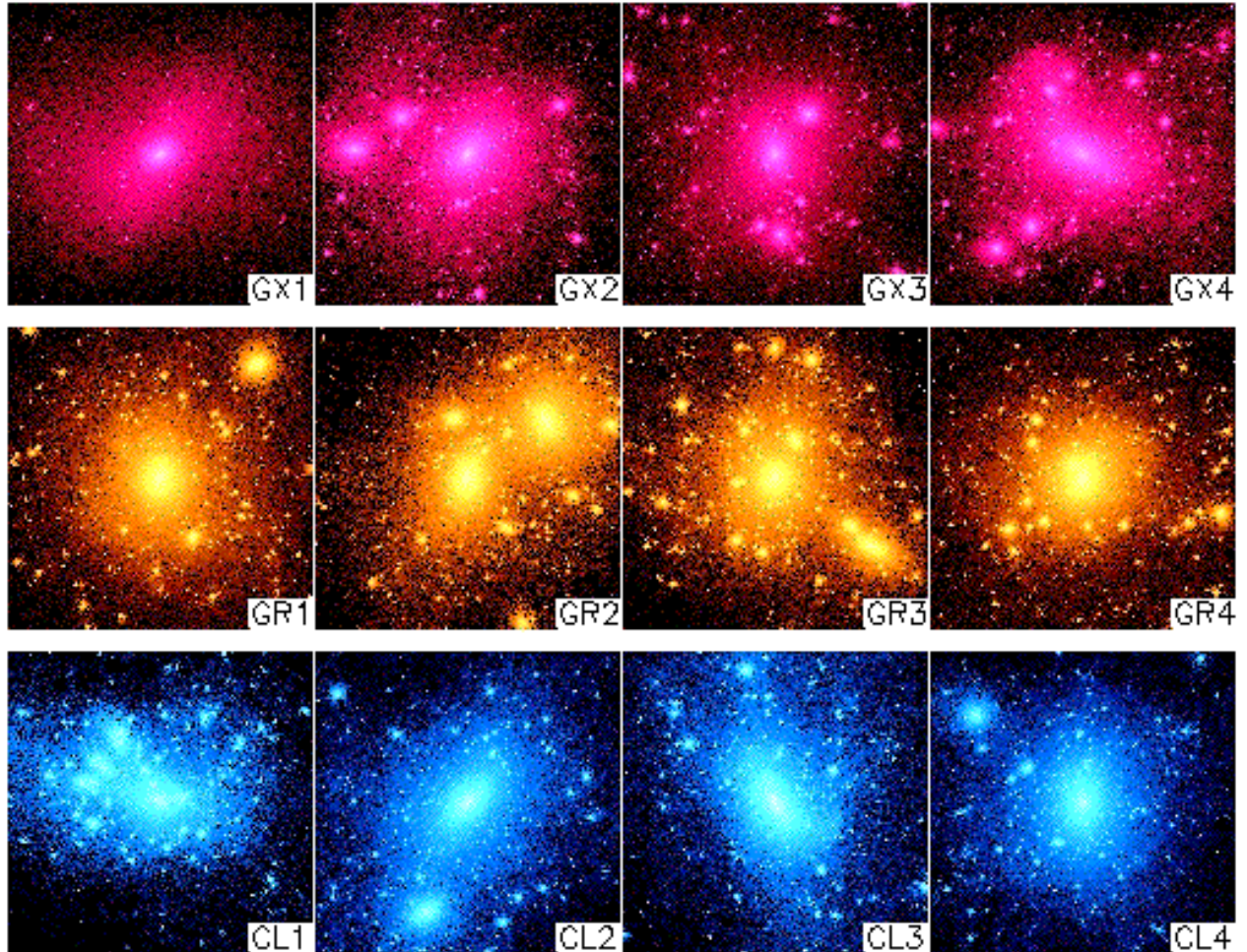


Fig. 1.— Snapshots of the simulated halos at $z = 0$. Left, middle and right panels display the halos of galaxy, group and cluster masses, respectively (see Table 1). The size of each panel corresponds to $2r_{\text{vir}}$ of each halo.

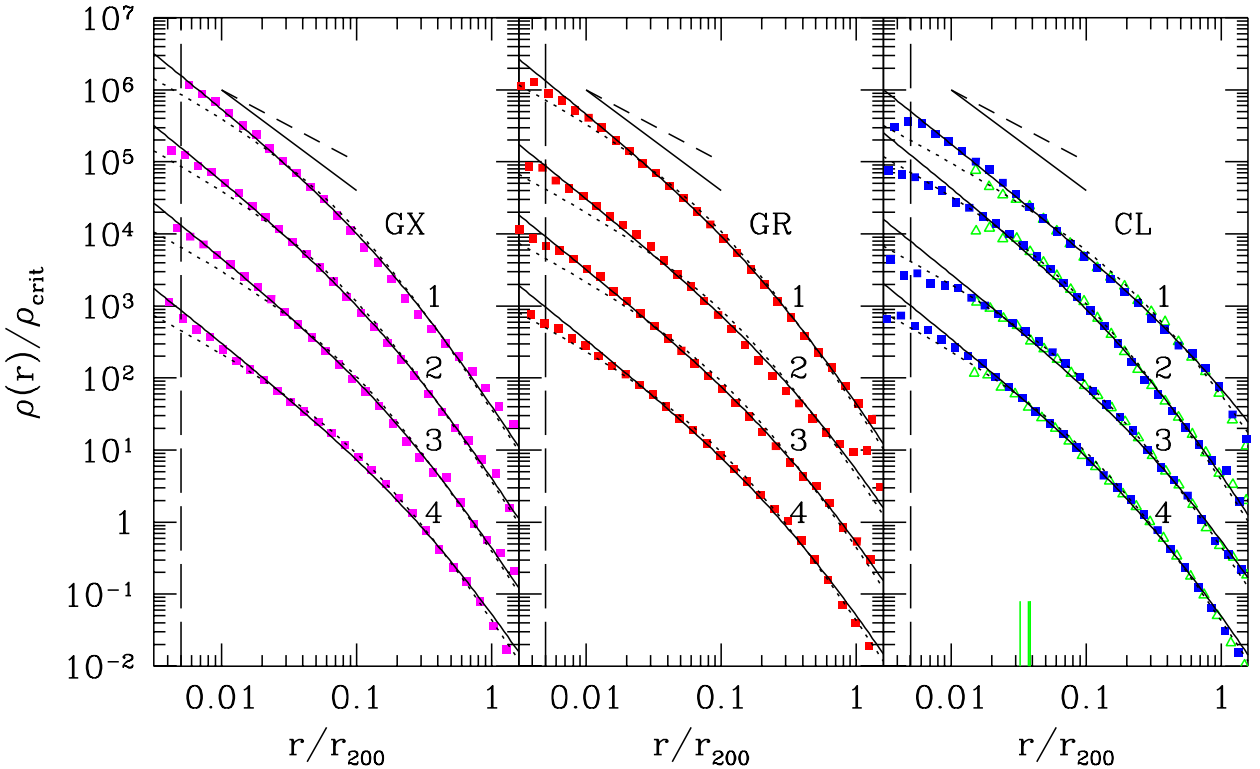


Fig. 2.— Spherically-averaged radial density profiles of the simulated halos of galaxy (*left*), group (*middle*), and cluster (*right*) masses. The solid and dotted curves represent fits to the proposed profile of Moore et al. (1999) and of NFW, respectively. For reference, we also show $\rho(r) \propto r^{-1}$ and $r^{-1.5}$ in dashed and solid lines. The vertical dashed lines indicate the force softening length which corresponds to our resolution limit. The open triangles in the right panel show the results for the corresponding halos in the lower-resolution cosmological simulation, and the long ticks at the bottom mark the force softening of the cosmological simulation. For the illustrative purpose, the values of the halo densities are multiplied by 1, 10^{-1} , 10^{-2} , 10^{-3} from top to bottom in each panel.

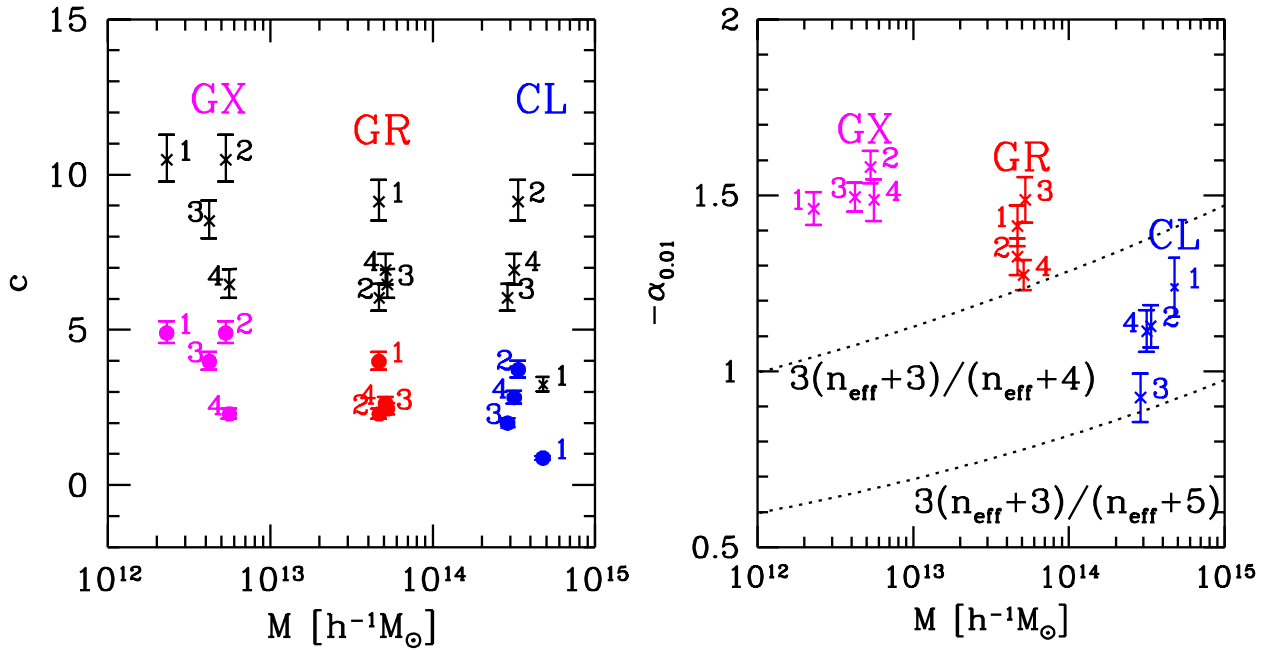


Fig. 3.— *Left panel*: the concentration parameters for each halo for the Moore et al. (1999) form (filled circles) and for the NFW form (crosses). Numbers labeling each symbol correspond to the halo ID in Table 1. *Right panel*: Power-law index of the inner region ($0.007 < r/r_{200} < 0.02$) as a function of the halo mass. The upper and lower dotted curves indicate the predictions of Hoffman & Shaham (1985) and Syer & White (1996), respectively.